

# 2–18-GHz Dispersion Measurements on 10–100- $\Omega$ Microstrip Lines on Sapphire

TERENCE C. EDWARDS AND ROGER P. OWENS

**Abstract**—Dispersion measurements on microstrip lines with characteristic impedances between 10 and 100  $\Omega$  are described, covering the frequency range 2–18 GHz. Single-crystal sapphire cut with a specified crystal orientation was used as the substrate material. Microstrip effective permittivities were calculated from the resonant frequencies of open-ended straight resonators using a technique which eliminated end-effect. The experimental results are compared with some recent dispersion theories. An empirical dispersion formula is independently developed, and is shown to provide well-fitting curves for all the measured dispersion results.

## I. INTRODUCTION

THE accurate design of microstrip circuits requires comparably accurate and reliable information on the dispersive behavior of the microstrip lines to be used. Currently available information on this behavior is incomplete. Experimentally, dispersion at frequencies above about 12 GHz is rarely investigated, and the range of line impedances considered has also been rather restricted. Available theoretical predictions have therefore not been tested over sufficiently wide frequency and impedance ranges.

In this paper we present the results of an extensive experimental investigation into the dispersive nature of microstrip lines on 0.5-mm-thick 25-mm-square monocrystalline sapphire substrates. The frequency range is extended up to 18 GHz and a broad characteristic impedance ( $Z_0$ ) range, 10–100  $\Omega$ , is considered. Certain available theoretical treatments are also compared with our results; including the spectral domain analysis of Itoh and Mittra [1] and the analytical formulation due to Getsinger [2]. Each shows slight departure from the measured results over certain parts of the frequency range. An empirical formula tailored to the measured points is independently developed, and incidentally shown to work effectively for a high-purity alumina substrate with thickness differing from that of the sapphire.

## II. MEASUREMENT METHOD AND ACCURACY CONSIDERATIONS

We used resonance measurements to determine microstrip effective permittivities  $\epsilon_{\text{eff}}$  for a set of resonant frequencies  $f$ . The procedure was repeated for several microstrip width-to-substrate-height ratios ( $W/h$ ) between 0.1 and 10 to obtain a family of dispersion points covering the frequency range 2–18 GHz in each case. Measurements were originally made on ring resonators, but towards the

two extremes of the linewidth range we encountered difficulties associated with 1) curvature effects, 2) frequency pulling due to coupling problems, and 3) the manufacture and physical measurement of high-tolerance thin rings.

As a result there were unacceptable variations between  $\epsilon_{\text{eff}}$  results for nominally very similar rings, and they were abandoned in favor of end-fed open-ended straight resonators. These gave more repeatable results for all the microstrip lines studied. The manufacturing and measurement difficulties were greatly eased, and it was possible to obtain adequate coupling without pulling the resonant frequency. End-effect was eliminated by working with pairs of straight resonators, nominally of identical width  $W$  and with identical coupling gaps  $g$ , but with physical lengths chosen so that the  $n$ th-order resonant frequency of the shorter resonator  $f_1$  corresponded very closely with the  $2n$ th-order resonance of the longer resonator  $f_2$ . The physical lengths were, respectively,  $l_1$  and  $l_2$ . Suppose  $l_e$  represents the sum of the coupling-gap end-effect length  $l_g$  and the open-line end-effect length  $l_0$  [3] and that  $l_e$  is the same for each resonator. The following equations can then be simply derived from the resonance conditions for each resonator [4]:

$$\epsilon_{\text{eff}} = \left[ \frac{nc(2f_1 - f_2)}{2f_1 f_2 (l_2 - l_1)} \right]^2 \quad (1)$$

and

$$l_e = \frac{f_2 l_2 - 2f_1 l_1}{(2f_1 - f_2)} \quad (2)$$

where  $c$  is the velocity of light.

Equations (1) and (2) hold provided both  $\epsilon_{\text{eff}}$  and  $l_e$  may be regarded as constant between  $f_1$  and  $f_2$ . We make  $l_2 \approx (2l_1 + l_e)$  to ensure that  $f_1$  and  $f_2$  are close. Equal coupling gaps are essential because  $l_g$ , and hence  $l_e$ , is dependent upon  $g$  [3]. This approach assumes that  $l_e$  is independent of the resonator length. There is evidence that this may not necessarily be true [5], but for a substrate with relative permittivity comparable to sapphire, data are only available for  $h = 1.27$  cm and  $W = 2$  cm. A scaling exercise has been carried out on Itoh's results which shows that all the resonators used in this study lie in the region where  $l_e$  is essentially constant.

The special requirements arising from this method are that, for each set of results, a pair of resonators must be made with identical widths and coupling gaps. They may both lie on a single substrate, or each may occupy one of a pair of substrates with very closely matched thicknesses, in order to accommodate a long resonator across a diagonal or to avoid resonator interaction. These requirements were

Manuscript received January 17, 1975; revised January 26, 1976.

The authors are with the Department of Electrical and Electronic Engineering, Royal Military College of Science, Shrivenham, Swindon, Wilts., England.

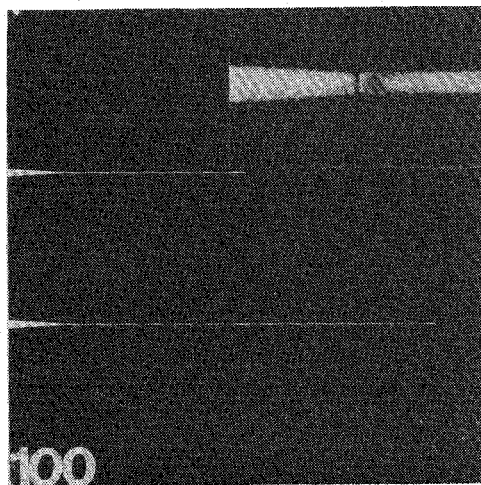
Fig. 1. 103- $\Omega$  resonator pair, with inset showing gap region.

TABLE I

Line No.	1	2	3	4	5	6	7	8	9	10	11
W, mm	4.490	2.445	1.921	1.068	0.642	0.415	0.275	0.178	0.111	0.073	0.050
h, mm	0.491	0.492	0.512	0.496	0.510	0.507	0.502	0.480	0.507	0.502	0.496
$\epsilon_{req}$	11.50	11.43	11.39	11.29	11.18	11.08	10.99	10.91	10.82	10.76	10.73
$\epsilon_{eo}$	9.733	9.057	8.732	8.108	7.594	7.263	7.019	6.832	6.640	6.524	6.448
$Z_0$ , ohms	10.03	16.53	20.46	30.05	41.29	51.24	60.98	70.64	83.86	94.26	103.58

achieved even for the narrowest resonators with  $W = 50 \mu\text{m}$ ,  $g = 10 \mu\text{m}$ , and lengths  $l_1 = 9.4 \text{ mm}$  and  $l_2 = 19.2 \text{ mm}$ . Fig. 1 is a photograph of this particular resonator pair, with an inset enlargement of the gap region. Additional values of  $\epsilon_{eff}$  were obtained from the odd-mode resonances of the longer resonators using

$$\epsilon_{eff} = \left[ \frac{nc}{2f_2(l_2 + l_e)} \right]^2 \quad (3)$$

where  $l_e$  may be interpolated between the values calculated from (2). In fact  $l_e$  was found to be substantially independent of frequency for most resonator pairs. Measurements were made using a network analyzer and a frequency counter with a repeatability of  $< \pm 2 \text{ MHz}$ . It was essential to have accurate measurements of resonator lengths (to  $\pm 5 \mu\text{m}$ ) and widths (to  $\pm 1 \mu\text{m}$ ) and to be sure that the coupling gaps were equal to within  $\pm 1 \mu\text{m}$ . The substrate thickness  $h$  not only governs the  $W/h$  ratio but also influences the dispersive behavior, particularly for wide lines, so it was also necessary to measure this parameter to  $\pm 5 \mu\text{m}$  in  $500 \mu\text{m}$ .

### III. DERIVATION OF QUASI-STATIC PARAMETERS OF EXPERIMENTAL MICROSTRIP LINES

Before comparing the experimental results with theoretical dispersion curves, it is necessary to establish the substrate relative permittivity  $\epsilon_r$  and, for each microstrip line, the low-frequency (LF) limit of microstrip effective permittivity  $\epsilon_{eo}$ . In practice,  $\epsilon_r$  is normally obtained from a separate experiment, then knowing  $W/h$  for the line, both  $\epsilon_{eo}$  and  $Z_0$  may be computed from available quasi-static microstrip

analysis theories [6]–[8]. The situation with monocrystalline sapphire substrates is complicated by the fact that the material is uniaxially anisotropic. All our substrates are cut with the crystal  $C$  axis perpendicular to the microstrip ground plane. The material permittivity is then constant everywhere in the plane of the substrate, and the microstrip line behavior is unaffected by its orientation in this plane. The quasi-static behavior of microstrip on sapphire cut with this particular  $C$ -axis orientation is dealt with theoretically in another paper [9]. It is shown there that the conventional quasi-static microstrip theories are applicable provided that  $\epsilon_r$  is replaced by a parameter called the equivalent isotropic-substrate relative permittivity  $\epsilon_{req}$ , which is a function of  $W/h$ . In Table I are listed the  $W$  and  $h$  measurements of the experimental microstrip lines and the corresponding values of  $\epsilon_{req}$  computed from  $W/h$  as described in [9], using  $\epsilon_{\perp} = 9.40$  and  $\epsilon_{\parallel} = 11.60$  as the principal relative permittivities of sapphire. In addition, the parameters  $\epsilon_{eo}$  and  $Z_0$  computed from Bryant and Weiss theory [7], [8] are tabulated.

### IV. COMPARISON OF EXPERIMENTAL RESULTS WITH SELECTED DISPERSION THEORIES

The experimental results for all measured lines are shown in Fig. 2, each set being identified by its line number. The  $\epsilon_{eo}$  values given in Table I are also plotted and they fit in quite well with the trend of the  $\epsilon_{eff}$  results at low frequencies, allowing for the fact that error bounds of up to 0.5 percent should be placed on each value of  $\epsilon_{req}$  [9]. This is a good indirect experimental check on the theoretical predictions of [9].

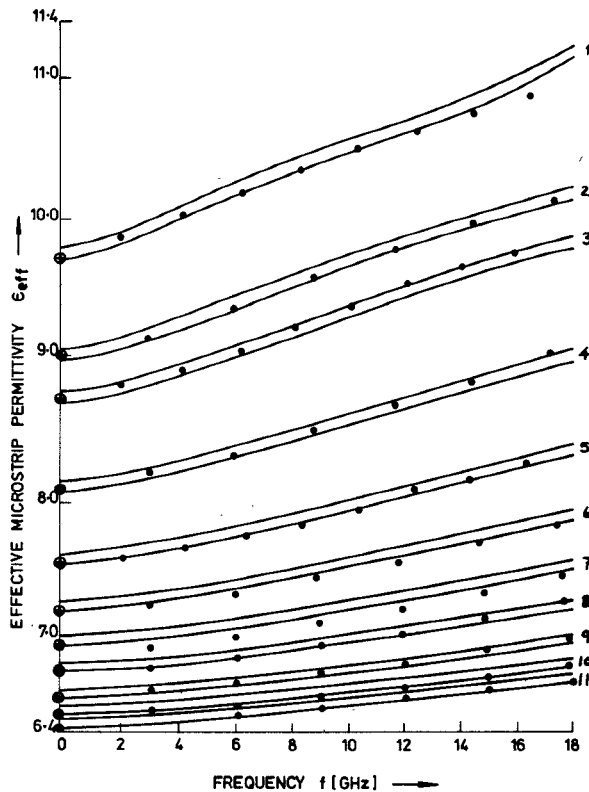


Fig. 2. Effective microstrip permittivity versus frequency. • Experimental results. + Predicted  $\epsilon_{eo}$  results [8]. Continuous curves from Itoh theory [1]. Double lines represent  $\epsilon_{req} \pm 0.05$ .

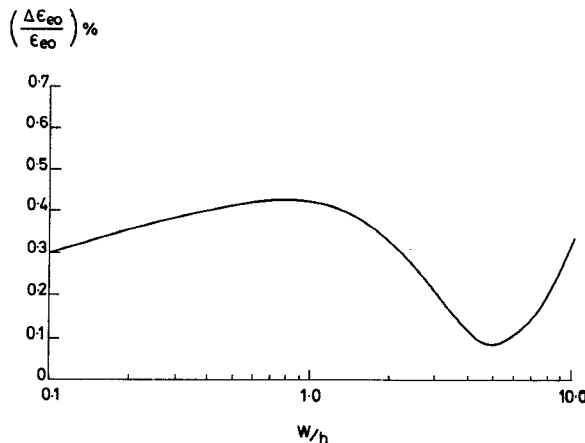


Fig. 3. Difference between Itoh predictions and Bryant and Weiss calculations of  $\epsilon_{eo}$  plotted against  $W/h$ .

A rigorous theoretical analysis of microstrip dispersion using a spectral domain approach has recently been carried out for microstrip in a conducting box [1]. Apart from box size, the data required for calculation of  $\epsilon_{eff}$  down to very low frequencies, are:  $W$ ,  $h$ , and  $\epsilon_{req}$ . These data, listed in Table I, have been applied to a computer program kindly supplied by Dr. T. Itoh, which implements the theory of [1]. For each line, the box size was increased until further increase had a negligible effect on the computed  $\epsilon_{eff}$  values. Fig. 2 shows the continuous curves thus generated, which are drawn in pairs in this instance, representing  $\epsilon_{req}$  (from Table I)  $\pm 0.05$  to account for the error bound previously mentioned. For many lines the curves are in very good

agreement with the measurements, although for the narrower lines it is the lower bound curve which best fits the points, and for lines 6 and 7, for example, the points lie even below this curve. This displacement may be partly due to the slight discrepancy between the values of  $\epsilon_{eo}$  calculated from quasi-static theory (given in Table I) and the values predicted by the Itoh and Mittra theory. This causes the curves of Fig. 2 to fall less sharply at their low-frequency ends than might be expected. The difference involved is less than 0.5 percent and it is plotted in Fig. 3 as a percentage deviation from the Bryant and Weiss [7], [8] quasi-static value versus  $W/h$ . If Wheeler theory is used [6], the discrepancy rises to almost 1 percent around  $W/h = 0.6$ .

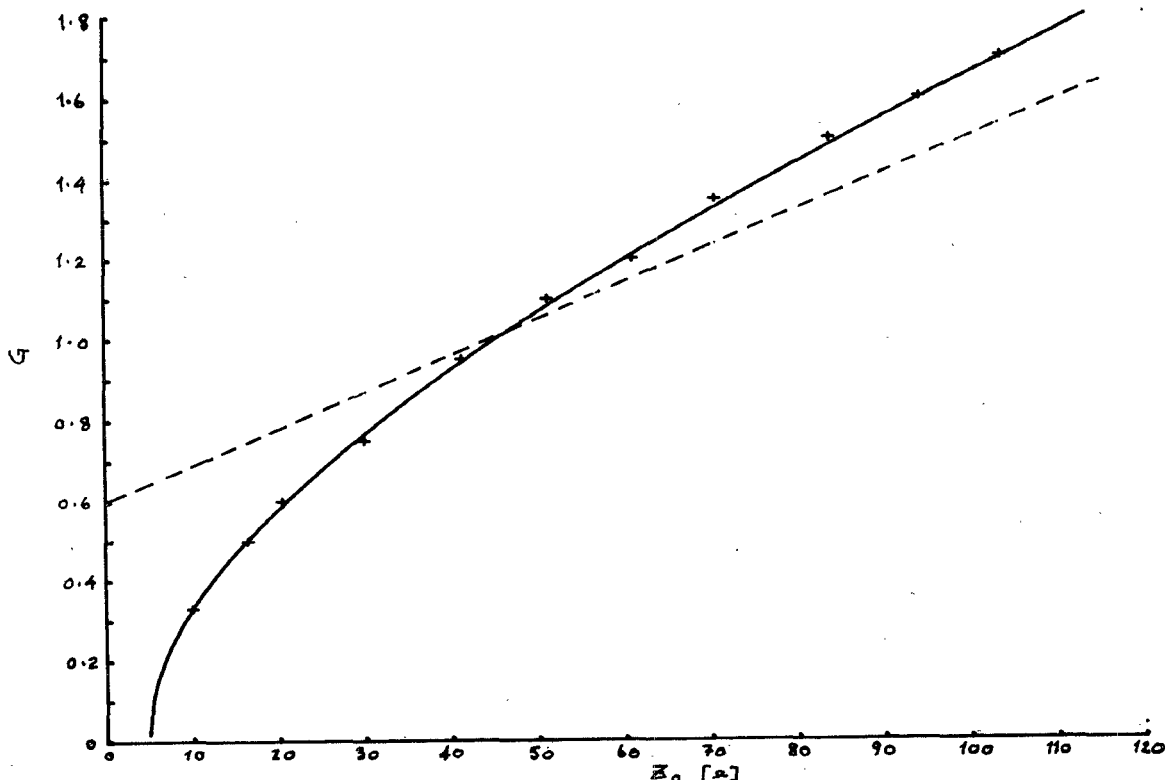


Fig. 4. Getsinger  $G$  parameter versus  $Z_0$ . + Optimized using measured dispersion curves. — Plotted from (7). —— Plotted from (6).

For computer-aided design purposes, analytical formulas such as those published by Getsinger [2] and Carlin [10], are of particular value. The Getsinger formula is

$$\epsilon_{\text{eff}} = \epsilon_{\text{req}} - \frac{(\epsilon_{\text{req}} - \epsilon_{e0})}{1 + G(f/f_p)^2} \quad (4)$$

where

$$f_p = \frac{Z_0}{2\mu_0 h} \quad (5)$$

and  $\mu_0$  is the free-space permeability. The parameter  $G$  is purely empirical, thereby giving some flexibility to the formula.  $G$  is dependent mainly on  $Z_0$  but also on  $h$ , and Getsinger deduced from measurements of ring resonators on alumina that

$$G = 0.6 + 0.009Z_0 \quad (6)$$

when  $h$  is 0.635 mm.

The range of the present measurements, the method employed, and the different substrate thickness, required that a new value of the  $G$ -factor should be determined by curve fitting to each set of experimental results. Only the measured results were used in the curve fitting. For each line  $\epsilon_{\text{req}}$  was allowed to deviate from the value given in Table I if necessary, so that  $\epsilon_{e0}$  could also deviate according to the quasi-static relationship between the two permittivities. The resulting optimized values of  $G$  are plotted against  $Z_0$  in Fig. 4. The equation

$$G = \left[ \frac{Z_0 - 5}{60} \right]^{1/2} + 0.004Z_0 \quad (7)$$

is plotted as a continuous curve in the figure and is seen to fit the optimized points very well. The Getsinger expression (6) for  $G$  is also plotted for comparison. There is clearly a considerable difference between the two curves, particularly at the low-impedance end of the figure.

The continuous curves of Fig. 5 were drawn using the Getsinger formula with the new expression for  $G$ . The broken curves *a* drawn in Fig. 5 for several representative lines were produced using  $G$  calculated from (6). As the line impedance falls, these curves are seen to deviate progressively more at the higher frequencies as the difference between the  $G$ -factors increases.

Selected curves using the theory of Carlin [10] are also shown as curves *b* in Fig. 5. This theory calculates  $\epsilon_{\text{eff}}$  from an equation of the form

$$\epsilon_{\text{eff}} = \epsilon_{e0} + \frac{(\epsilon_{\text{req}} - \epsilon_{e0})Af^2}{1 + \sqrt{Af^4 + 1}} \quad (8)$$

where  $A$  is a function of  $Z_0$  and  $h$  which can be derived from [10]. No attempt was made to optimize  $A$  for these curves, which also rise sharply at the high-frequency ends for the low-impedance lines, but it is anticipated that a similar improvement in the fit could be obtained.

## V. DISCUSSION OF RESULTS

The analytical equation of Getsinger provides a fairly accurate prediction of microwave dispersion over the wide range of frequencies and line impedances covered by the present measurements, provided that the proper expression for the parameter  $G$  is used. In order to obtain a good overall fit to the measured points, however, the curves of

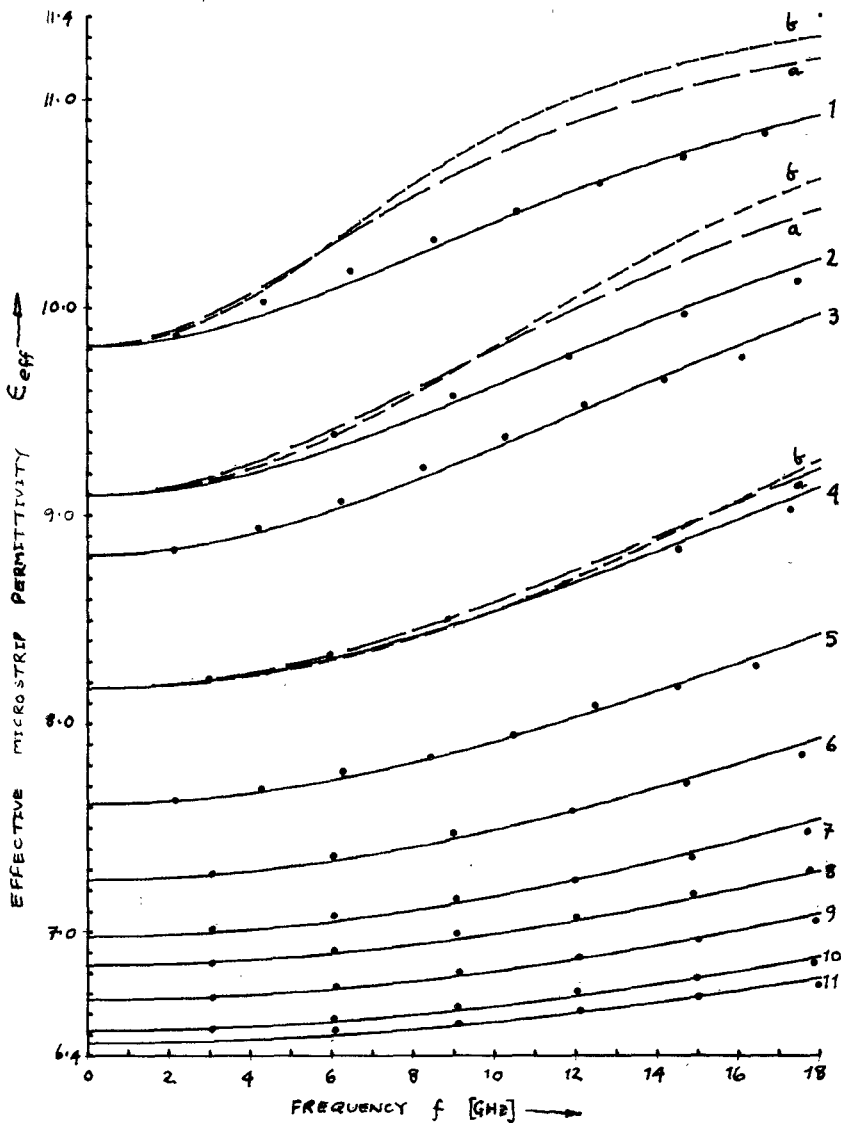


Fig. 5. Effective microstrip permittivity versus frequency. • Experimental results. — Getsinger curves using (7) for  $G$ . Curves  $a$ , Getsinger curves using (6) for  $G$ . Curves  $b$ , Carlin curves using (8) with  $A$  values from [10].

Fig. 5 in general fall slightly below the points at the lower end of the frequency range, but rise above them at the high-frequency end. There is, therefore, scope for an alternative analytical dispersion equation which can take this consistent discrepancy into account by including higher order powers of frequency in the expression for the dependent variable  $\epsilon_{\text{eff}}$ .

In its most general form, such an equation will be as follows:

$$\epsilon_{\text{eff}} = \epsilon_{\text{req}} - \frac{(\epsilon_{\text{req}} - \epsilon_{\text{e0}})}{1 + P} \quad (9)$$

where  $P$  is a polynomial

$$P = a_2 f^2 + a_3 f^3 + \cdots + a_n f^n. \quad (10)$$

This equation obeys the three conditions 1)  $\epsilon_{\text{eff}} = \epsilon_{\text{e0}}$  when  $f = 0$ ; 2)  $d(\epsilon_{\text{eff}})/df = 0$  when  $f = 0$ ; 3)  $\epsilon_{\text{eff}} \rightarrow \epsilon_{\text{req}}$  as  $f \rightarrow \infty$ . The coefficients  $a_n$  must be functions of  $h$  and  $Z_0$  to allow for the dependence of dispersion on these two

microstrip parameters. It will be noted that if  $a_2 = G/f_p^2$  and  $a_n = 0$  ( $n > 2$ ), Getsinger's equation is recovered. Similarly, after rearrangement of (9) into the form of (8), it may be seen that if  $A^2 f^4 \gg 1$ , Carlin's formula is obtained by putting  $a_2 = A$  and  $a_n = 0$  ( $n > 2$ ). Thus (9) is a natural progression from (4) and (8) involving one or more extra empirical parameters in addition to  $G$  or  $A$ .

It is only necessary to include the extra term  $a_3 f^3$  in the polynomial to obtain a good fit to the experimental results. A simple relationship between the optimized coefficients  $a_2$  and  $a_3$  and  $h/Z_0$  for each line was observed, and the final form of the polynomial  $P$  to be used in (9) was found to be

$$P = (h/Z_0)^{1.33} [0.43f^2 - 0.009f^3] \quad (11)$$

where  $h$  is in millimeters and  $f$  is in gigahertz.

Fig. 6 shows the curves generated using this polynomial, illustrating the very close agreement with the experimental results. The empirical equations clearly cover a wide range

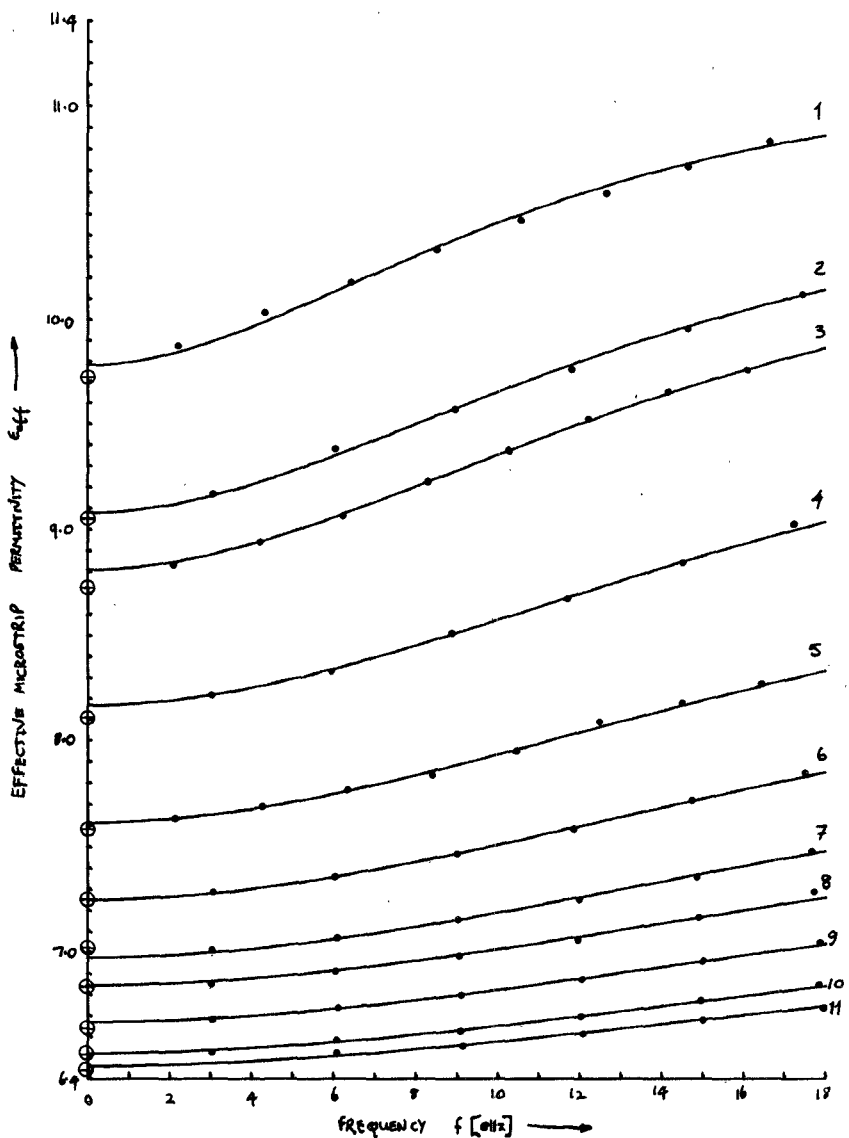


Fig. 6. Effective microstrip permittivity versus frequency. • Experimental results. + Predicted  $\epsilon_{e0}$  results [7]. Continuous curves from combined (9) and (11).

TABLE II

Line Number	1	2	3	4	5	6	7	8	9	10	11
$\epsilon_{req}$ (theoretical)	11.50	11.43	11.39	11.29	11.18	11.08	10.99	10.91	10.82	10.76	10.73
$\epsilon_{req}$ (analytical formula)	11.56	11.46	11.50	11.38	11.21	11.06	10.92	10.93	10.87	10.75	10.75

of line impedances, but the validity of the  $h$ -dependence has not been checked with sapphire substrates of different thickness. As was also observed with the Getsinger curves, the  $\epsilon_{e0}$  and  $\epsilon_{req}$  values predicted by the curves of Fig. 6 are in general slightly higher than those obtained theoretically. Table II shows the relative values of  $\epsilon_{req}$ . The differences involved are quite small and are mostly accounted for by the  $\pm 0.05$  error on the theoretical  $\epsilon_{req}$  values. An alternative explanation is that, as predicted by the Itoh curves (Fig. 2), the slope  $d(\epsilon_{eff})/df$  may remain fairly constant down to

very low frequencies, particularly for wider lines. In contrast the analytical formulas predict a square-law relationship below about 3 GHz and therefore a somewhat higher  $\epsilon_{e0}$  on the fitted curve. The fact that the discrepancy increases for wider lines lends support to this explanation.

The polynomial formula clearly works up to 18 GHz, but at 31.85 GHz,  $dP/df$ , and hence  $d(\epsilon_{eff})/df$ , are maximized, and above this frequency the formula is ill-behaved. This expression should therefore be used with caution at frequencies much above 18 GHz.

TABLE III

Line number	W mm	$\epsilon_{eo}$	$Z_0 \Omega$	Getsinger G-factor
1	1.450	7.354	31	0.7
2	0.585	6.736	51	0.95
3	0.260	6.420	71	1.15

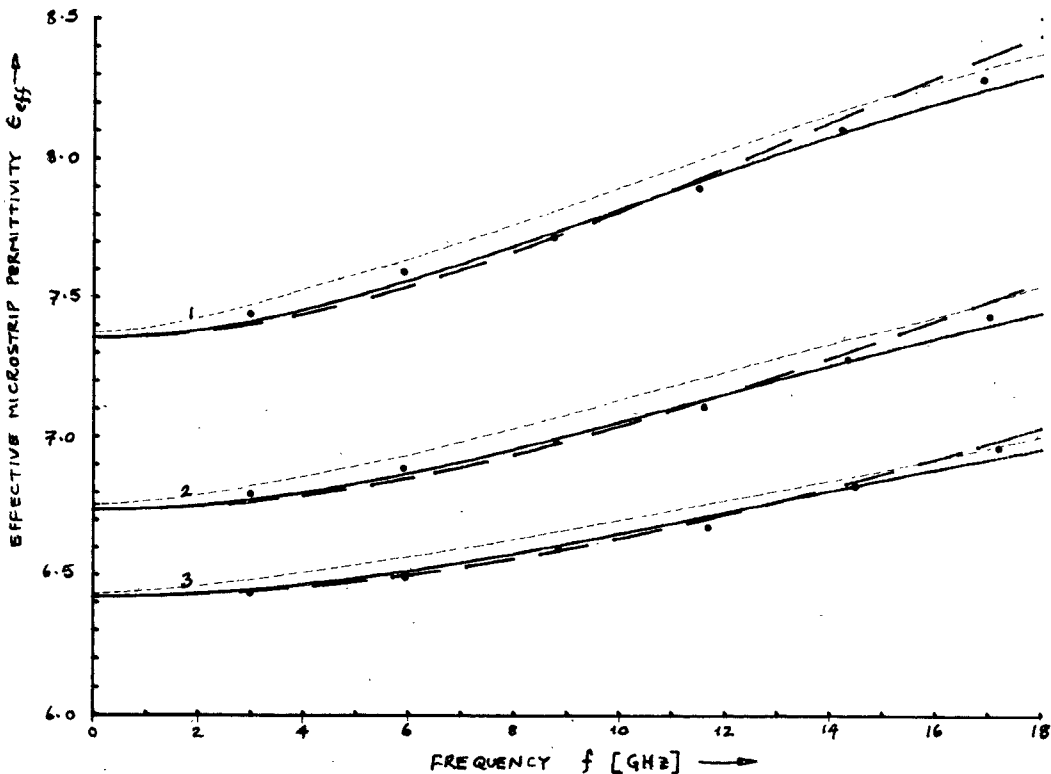


Fig. 7. Dispersion results for microstrip lines on alumina. • Experimental results. — Polynomial curves [(9) and (11)]. - - - Getsinger curves (optimized  $G$ -factor). - - - Itoh curves. For line parameters see Table III.

The influence of the sapphire substrate anisotropy on dispersion has not been taken into account, although it might be argued that any discrepancy between our results and the theoretical predictions could be attributed at least partly to such an effect. Intuitively, one might expect that the normal increase in  $\epsilon_{eff}$  with frequency would be opposed by some decrease due to a progressively larger component of electric field in the plane of the air-dielectric interface, where the sapphire permittivity has the lower value  $\epsilon_{\perp}$ . The determination of the magnitude of this effect would be a subject for separate study, but the following discussion of measurements with microstrip resonators on alumina is relevant to this problem.

Preliminary experiments have been conducted using high-purity alumina substrates ("Alsimag" 805) with the quoted permittivity  $\epsilon_r = 10.1$  (at 1 MHz). Table III lists the parameters of each line. The substrate height was 0.65 mm. The value  $\epsilon_r = 10.15$  was obtained by curve fitting using the analytical formulas, and  $\epsilon_{eo}$  and  $Z_0$  follow from this. The  $G$ -factors required to obtain a good fit using the Getsinger formula are included in the table, and it is seen that these differ from values calculated using either (6) or (7).

Fig. 7 shows the measured results, together with curves using Itoh theory, the Getsinger equation with optimized  $G$ ,

and the polynomial expression. The latter results provide quite satisfactory confirmation that the dispersion formula using (9) and (11) is applicable to thicker alumina substrates without further change in the polynomial parameters. The behavior of the Itoh and Getsinger curves is similar to that observed earlier for microstrip on sapphire. In addition, the measured high-frequency dispersion behavior closely resembles that observed using sapphire substrates, strongly suggesting that the effect of sapphire anisotropy on dispersion is very small.

## VI. CONCLUSIONS

By careful measurements we have obtained repeatable and accurate dispersion data for open microstrip lines on sapphire substrates in the characteristic impedance range  $10 < Z_0 < 100 \Omega$ , and for frequencies up to 18 GHz. Dispersion predictions using the theory of Itoh and Mittra have been shown to compare very well with experiment. There is, however, a slight discrepancy at frequencies approaching the LF limit when compared with previously accepted accurate quasi-static calculations [7]. The theory has the advantage that it does not involve any empirical factor and only the parameters  $W$ ,  $h$ , and  $\epsilon_r$  are required. Despite the necessity for lengthy computation it is therefore

particularly suitable for predicting the dispersion of lines on a substrate with arbitrary height and permittivity.

The Getsinger analytical expression has been shown to be capable of fitting experimental results quite well, but only after suitable tailoring of the empirical parameter  $G$ . The limited results for microstrip on alumina suggest that for each new substrate the  $G$  parameter must be experimentally determined to account for different substrate height and permittivity. This limits the potential of the formula for predicting the dispersion of an arbitrary line on an arbitrary substrate. Similar limitations probably apply to the new dispersion equation involving the polynomial, which was developed to predict the fine detail of the experimental  $\epsilon_{eff}$  versus frequency curves and includes two empirical parameters. The alumina results, however, seem to indicate that this formula is not too sensitive to changes in substrate parameters.

When working with alumina, the uncertain electrical properties, including possible variable bulk permittivity with frequency [11] and unpredictable anisotropy [12], add to the difficulties of precision measurement. It is felt that in these experiments, the use of sapphire as the substrate, with its repeatable and established electrical properties, has been a distinct advantage in ensuring that accurate measurements of microstrip characteristics were not unduly influenced by variable substrate material behavior.

#### ACKNOWLEDGMENT

This work was done as part of an M.I.C. research program directed by Prof. M. H. N. Potok whom, together with Dr. J. E. Aitken, we wish to thank for several valuable

discussions. Mrs. C. Garrett and V. Hartley are also thanked for their consistently high-grade microcircuit fabrication, under the general supervision of E. H. England. We are particularly grateful to Dr. T. Itoh for a copy of his microstrip dispersion program.

#### REFERENCES

- [1] T. Itoh and R. Mittra, "Spectral-domain approach for calculating the dispersion characteristics of microstrip lines," *IEEE Trans. Microwave Theory and Tech.*, vol. MTT-21, pp. 496-499, July 1973.
- [2] W. J. Getsinger, "Microstrip dispersion model," *IEEE Trans. Microwave Theory and Tech.*, vol. MTT-21, pp. 34-39, Jan. 1973.
- [3] J. G. Richings, "An accurate experimental method for determining the important properties of microstrip transmission lines," *The Marconi Review*, pp. 209-216, Fourth Quarter, 1974.
- [4] J. Deutsch and H. J. Jung, "Measurement of the effective dielectric constant of microstrip lines in the frequency range from 2 GHz to 12 GHz," *NTZ*, vol. 12, pp. 620-624, 1970.
- [5] T. Itoh, "Analysis of microstrip resonators," *IEEE Trans. Microwave Theory and Tech.*, vol. MTT-22, pp. 946-952, Nov. 1974.
- [6] H. A. Wheeler, "Transmission-line properties of parallel strips separated by a dielectric sheet," *IEEE Trans. Microwave Theory and Tech.*, vol. MTT-13, pp. 172-188, March 1965.
- [7] T. G. Bryant and J. A. Weiss, "Parameters of microstrip transmission lines and of coupled pairs of microstrip lines," *IEEE Trans. Microwave Theory and Tech.*, vol. MTT-16, pp. 1021-1027, Dec. 1968.
- [8] T. C. Cisco, "Design of microstrip components by computer," NASA Contractor Report CR-1982, March 1972, Program C267.
- [9] R. P. Owens, J. E. Aitken, and T. C. Edwards, "Quasi-static characteristics of microstrip on an anisotropic sapphire substrate," this issue, pp. 499-505.
- [10] H. J. Carlin, "A simplified circuit model for microstrip," *IEEE Trans. Microwave Theory and Tech.*, vol. MTT-21, pp. 589-591, Sept. 1973.
- [11] S. Arnold, "Dispersive effects in microstrip and alumina substrates," *Electronics Letters*, vol. 5, no. 26, pp. 673-674, 27 Dec. 1969.
- [12] J. W. C. van Heuven and T. H. A. M. Vlek, "Anisotropy in alumina substrates for microstrip circuits," *IEEE Trans. Microwave Theory and Tech.*, vol. MTT-20, pp. 775-777, Nov. 1972.